

(c) PP electrochemistry is much more facile on Pt than on glassy carbon. This conclusion is also supported by other data not included in Table II.

(d) The anodic wave is more susceptible to kinetic limitations than is the cathodic wave. Thus, as the scan speed or the film thickness is increased and ΔE_p increases, E_{pa} changes more than E_{pc} , and so E'_{app} moves to more anodic potentials.

(e) Films prepared in a neutral melt exhibit more facile electrochemistry in a 0.8:1 melt than in CH_3CN .

(f) Films prepared in CH_3CN show very poor electrochemistry in a 0.8:1 melt when compared to similar films prepared in the neutral melt. In CH_3CN they are similar to films prepared in the neutral melt.

(g) Peak positions are poorly reproducible. This is probably due to different degrees of swelling and hence variable kinetics and thermodynamics.

It should be noted that the differences between CH_3CN and the melt may be in part due to the different temperatures employed for experiments in the two solvents.

Conclusions

Polypyrrole films can be prepared in molten BuPyAlCl_4 and the electrochemistry of such films in 0.8:1 mol ratio AlCl_3 : BuPyCl melt appears to be more facile than that of PP films prepared in CH_3CN . The films prepared in the melt are conducting when oxidized and are potentially useful electrode materials. Their charge storing properties are superior to those of previously described PP films.

Further work concerning the nature of the electrochemical reaction of PP and the conductivity of films prepared in molten salts is in progress.

Acknowledgment. This work was supported in part by the Air Force Office of Scientific Research and the Office of Naval Research.

Registry No. AlCl_3 , 7446-70-0; Pt, 7440-06-4; C, 7440-44-0; BuPyCl , 1124-64-7; ferrocene, 102-54-5; pyrrole, 109-97-7; polypyrrole, 30604-81-0.

Calculation of NMR Spin-Spin Coupling Constants Using the Extended Hückel Molecular Orbital Method

Frank A. A. M. de Leeuw, Cornelis A. G. Haasnoot,[†] and Cornelis Altona*

Contribution from the Gorlaeus Laboratories, University of Leiden, 2300 RA Leiden, The Netherlands. Received July 25, 1983

Abstract: NMR spin-spin coupling constants are calculated by means of the extended Hückel molecular orbital theory (EHMO). The contributions to the coupling constant from orbital, spin-dipolar, and Fermi-contact interactions are included. By use of the Ruedenberg expansion the evaluation of multicenter integrals in the orbital and spin-dipolar contributions is circumvented. For the Fermi-contact contribution all one- and two-center integrals are retained. It is shown that a reparametrization of the EHMO parameters results in quantitative agreement between experimental and calculated coupling constants. An optimization of the EHMO parameters upon a data set containing $^1J_{\text{CH}}$ and $^3J_{\text{HH}}$ couplings shows systematic deviations of the idealized regression line both for the $^1J_{\text{CH}}$ and for the $^3J_{\text{HH}}$ subset. The best results are obtained with a separate optimization of EHMO parameters for the subsets $^1J_{\text{CH}}$ and $^3J_{\text{HH}}$. With the use of these parameter sets, a host of experimental trends due to substituent effects or to stereochemical effects are reproduced. The use of the optimized parameters for $^1J_{\text{CH}}$ may be extended to the calculation of $^1J_{\text{CC}}$. The $^3J_{\text{HH}}$ parameter set allows the prediction of the dependence of gauche and trans couplings upon the electronegativity and orientation of substituents in 1,2-disubstituted ethane-like fragments.

One of the prime reasons for the success of NMR spectroscopy as a structural tool has been the application of spin-spin coupling constants to stereochemistry. As the magnitude of the coupling constants depends upon variety of molecular parameters, such as torsion angles, bond angles, bond lengths, substitution, etc., much attention has been given to their theoretical calculation¹ in order to derive useful relationships between coupling constants and molecular structure.

Theoretical investigation of coupling constants in small molecules is frequently carried out by means of ab initio methods. However, in conformational analysis one is usually interested in large-size molecules containing many heavy atoms. Then ab initio methods are too expensive, forcing the use of semiempirical methods. A comparison of the ability to reproduce experimental couplings by the most common semiempirical approaches (CNDO, INDO, and extended Hückel theory) can be found in ref 2-5.

In the present paper we investigate the calculation of coupling constants $^3J_{\text{HH}}$ and $^1J_{\text{CH}}$ with two objectives in mind: (i) the calculated coupling constants must be reliable, as demonstrated by a quantitative agreement with experimental data; (ii) the method used should be as economical as possible.

The first objective is necessary for a detailed theoretical investigation of the dependence of coupling constants upon stereochemical and/or substituent effects. The second objective makes it possible to study these effects in relatively large molecules. Moreover, with a fast and "simple" computational method, calculations can be performed on small-size computers.⁶

Attention is focused solely on the calculation of $^3J_{\text{HH}}$ and $^1J_{\text{CH}}$ because these types of couplings are important from the view of stereochemistry and conformational analysis. Geminal couplings of the type $^2J_{\text{HH}}$ and $^2J_{\text{CH}}$ were not included in the data set. Pilot calculations showed that, e.g., $^2J_{\text{HH}}$ depends markedly upon the H-C-H bond angle and upon the C-H bond distances, and in general these parameters are not known experimentally to a high degree of precision.

(1) See, for example: Kowalewski, J. *Prog. Nucl. Magn. Reson. Spectrosc.* **1977**, *11*, 1. Kowalewski, J. *Annu. Rep. NMR Spectrosc.* **1982**, *12*, 81.

(2) Armour, E. A. G.; Stone, A. J. *Proc. R. Soc. London, Ser. A* **1967**, *4302*, 25.

(3) de Jeu, W. H.; Bener, G. P. *Theor. Chim. Acta* **1969**, *13*, 349.

(4) Barbieri, G.; Benassi, R.; Lazzaretti, P.; Taddei, F. *Org. Magn. Reson.* **1975**, *7*, 563.

(5) André, J. M.; Nagy, J. B.; Derouane, E. G.; Fripiat, J. G.; Vercauteren, D. P. *J. Magn. Reson.* **1977**, *26*, 317.

(6) Osapay, K.; Farkas, M.; Vajda, M. *Comput. Chem.* **1976**, *1*, 125.

[†] Present Address: Department of Biophysical Chemistry, Toernooiveld, 6525 ED Nijmegen, The Netherlands.

The successful calculation of coupling constants depends upon the particular MO method chosen to find the MO coefficients and orbital energies. A comparison of the various approaches demonstrates that the extended Hückel molecular orbital method (EHMO) of Hoffmann⁷ is at least as reliable as the usual CNDO and INDO methods.^{4,5} In the original version of the EHMO model the eigenvalue problem is solved only once and the calculations take less computer time than INDO, CNDO, or MINDO. Therefore we investigate the scope of the EHMO method for the routine calculation of $^1J_{CH}$ and $^3J_{HH}$. It is well-known that the use of standard EHMO parameters yields calculated couplings which are grossly underestimated, although experimental trends are roughly reproduced. We wish to produce better agreement with experiment for a larger number of different types of compounds than was hitherto attained. This goal is realized by a reparametrization of the EHMO method.

Theory

Ramsey⁸ showed that the spin-spin coupling constant J_{AB} between the nuclei A and B may be written as the sum of three separate contributions, eq 1. The first term, the orbital con-

$$J_{AB} = J_{AB}^{\text{orb}} + J_{AB}^{\text{dip}} + J_{AB}^{\text{contact}} \quad (1)$$

tribution, describes the interaction between the nuclear magnetic moments and the orbital motion of the electrons. The second term, the spin-dipolar contribution, represents the dipole-dipole interaction between nuclear and electron spins. The third term gives the interaction between the nuclear and electron spins at the site of the nucleus and is called the Fermi-contact contribution.

Pople and Santry⁹ combined Ramsey's perturbation theory expressions with the LCAO-MO theory to obtain tractable equations for the different types of contributions. If one of the coupled nuclei is a proton, the orbital and spin-dipolar terms are relatively small in comparison to the Fermi-contact term. The latter is represented by eq 2 in which the various symbols are defined in ref 9. The spin-dipolar contribution is given by eq

$$J_{AB}^{\text{contact}} = -(8\beta/3)h\gamma_A\gamma_B \sum_i^{\text{occ}} \sum_j^{\text{unocc}} (\epsilon_i - \epsilon_j)^{-1} \sum_{\lambda\mu\nu\sigma} c_{i\lambda}c_{j\mu}c_{i\nu}c_{j\sigma} \langle \phi_\lambda | \delta(\bar{r}_A) | \phi_\mu \rangle \langle \phi_\nu | \delta(\bar{r}_B) | \phi_\sigma \rangle \quad (2)$$

3, using the usual summation convention for the tensor suffixes α and β . In isotropic solutions this contribution vanishes if one of the nuclei involved in the coupling is a proton. However, when both coupled nuclei possess valence orbitals of p or higher quantum number, the spin-dipolar term becomes important. The difficulties involved in calculating the multicenter integral in eq 3 can be

$$J_{AB}^{\text{dip}} = -\frac{4}{3}\beta^2(\hbar\gamma_A\gamma_B/2\pi) \sum_i^{\text{occ}} \sum_j^{\text{unocc}} (\epsilon_i - \epsilon_j)^{-1} \sum_{\lambda\mu\nu\sigma} c_{i\lambda}c_{j\mu}c_{i\nu}c_{j\sigma} \langle \phi_\lambda | r_A^{-5}(3r_{A\alpha}r_{A\beta} - r_A^2\delta_{\alpha\beta}) | \phi_\mu \rangle \langle \phi_\nu | r_B^{-5}(3r_{B\alpha}r_{B\beta} - r_B^2\delta_{\alpha\beta}) | \phi_\sigma \rangle \quad (3)$$

circumvented by means of the Ruedenberg expansion;¹⁰ the atomic orbitals ϕ_{Nk} located on an atom N are used as a basis to develop an atomic orbital ϕ_λ on any other atom

$$\phi_\lambda = \sum_k S_{\lambda k} \phi_{Nk}$$

In this way the multicenter integrals are written as a sum of one-center integrals. By writing

$$d_{iq} = \sum_p c_{ip} S_{pq}$$

the spin-dipolar contribution is given by eq 4.

The first term in eq 1, the orbital contribution, may be separated into two parts, eq 5 and eq 6, in which \bar{M}_A is the orbital angular

$$J_{AB}^{\text{dip}} = -\frac{8}{25}\beta^2(\hbar\gamma_A\gamma_B/2\pi) \sum_i^{\text{occ}} \sum_j^{\text{unocc}} (\epsilon_i - \epsilon_j)^{-1} \langle r_A^{-3} \rangle \langle r_B^{-3} \rangle \times \{4 \sum_\alpha d_{A\alpha i} d_{A\alpha j} d_{B\alpha i} d_{B\alpha j} + 3 \sum_{\alpha \neq \beta} d_{A\alpha i} d_{A\beta j} (d_{B\alpha i} d_{B\beta j} + d_{B\alpha j} d_{B\beta i}) - 2 \sum_{\alpha \neq \beta} d_{A\alpha i} d_{A\alpha j} d_{B\beta i} d_{B\beta j}\} \quad \text{where } \langle r_A^{-3} \rangle = \langle p_{A\alpha} | r^{-3} | p_{A\alpha} \rangle \quad (4)$$

$$J_{AB}^{\text{orb,a}} = \frac{\hbar}{2\pi} \gamma_A \gamma_B \left(\frac{4e^2}{3mc^2} \right) \sum_i^{\text{occ}} \sum_{\lambda\mu} c_{i\lambda} c_{i\mu} \left\langle \phi_\lambda \left| \frac{\bar{r}_A \bar{r}_B}{r_A^3 r_B^3} \right| \phi_\mu \right\rangle \quad (5)$$

$$J_{AB}^{\text{orb,b}} = (\hbar/2\pi) \gamma_A \gamma_B (-1/3\beta^2) \sum_i^{\text{occ}} \sum_j^{\text{unocc}} (\epsilon_i - \epsilon_j)^{-1} \sum_{\lambda\mu\nu\sigma} c_{i\lambda} c_{j\mu} c_{i\nu} c_{j\sigma} \langle \phi_\lambda | r_A^{-3} \bar{M}_A | \phi_\mu \rangle \langle \phi_\nu | r_B^{-3} \bar{M}_B | \phi_\sigma \rangle \quad (6)$$

momentum about nucleus A. The term given by eq 6 disappears if a proton is involved in the coupling. With the aid of the Ruedenberg expansion eq 5 may be evaluated¹⁰ to give eq 7. The

$$J_{AB}^{\text{orb,a}} = (\hbar/2\pi) \gamma_A \gamma_B (4e^2/3mc^2) \times \sum_i^{\text{occ}} \left\{ \sum_{\alpha\beta} \frac{1}{2} d_{A\alpha i} d_{A\beta i} \langle \phi_{A\alpha} | \theta_{AB} | \phi_{A\beta} \rangle + \sum_{\alpha\beta} \frac{1}{2} d_{B\alpha i} d_{B\beta i} \langle \phi_{B\alpha} | \theta_{AB} | \phi_{B\beta} \rangle \right\} \quad (7)$$

matrix elements $\langle \phi_{A\alpha} | \theta_{AB} | \phi_{A\beta} \rangle$ have been evaluated by McConnell,¹¹

$$\langle \phi_{A\alpha} | \theta_{AB} | \phi_{A\beta} \rangle = r_{AB}^{-3} \langle \phi_{A\alpha} | r_A^{-1} | \phi_{A\beta} \rangle - r_{AB}^{-2} \langle \phi_{A\alpha} | r_A^{-2} \cos(\bar{r}_A, \bar{r}_B) | \phi_{A\beta} \rangle$$

In general this term will be small because of its dependence on r_{AB}^{-3} . However, this term does not vanish, even for couplings involving only protons.

The evaluation of the second term of the orbital contribution is identical with that of the spin-dipolar contribution. One obtains eq 8.

$$J_{AB}^{\text{orb,b}} = (\hbar/2\pi) \gamma_A \gamma_B (-1/3\beta^2) \sum_i^{\text{occ}} \sum_j^{\text{unocc}} (\epsilon_i - \epsilon_j)^{-1} \langle r_A^{-3} \rangle \times \langle r_B^{-3} \rangle \sum_{\alpha \neq \beta} d_{A\alpha i} d_{A\beta i} (d_{B\alpha i} d_{B\beta j} - d_{B\beta i} d_{B\alpha j}) \quad (8)$$

Before the actual optimization of the EHMO parameters was carried out, the dependence of the calculated coupling constants upon the various approximations within the EHMO method was investigated. An outline of the computational details will be given.

In the calculation of MO coefficients and orbital energies, as well as in the coupling constant calculations, Slater-type orbitals are employed as a basis set. However, Slater-type orbitals cannot be used in the evaluation of the valence shell orbital densities at the nucleus, necessary in the calculation of the Fermi-contact contribution, owing to the improper behavior of the 2s-orbitals at the nucleus (the so-called Cusp problem). For this part of the calculation hydrogen-like orbitals may be adopted. However, preliminary calculations showed that the calculated coupling constants are highly dependent on the value of the effective nuclear charges. Therefore, it was decided to treat the orbital value at the nucleus ($\psi(0)$, defined as $\psi(0) = (\langle s_A | \delta(r_A) | s_A \rangle)^{1/2}$ as an adjustable parameter. The reason why the orbital value ($\psi(0)$) and not the spin density ($\psi^2(0)$) at the nucleus is chosen for this purpose lies in the calculation of the Fermi-contact contribution for which the two-center integrals are retained. It is then necessary to use the correct sign of $\psi(0)$; for second-row elements $\psi(0)$ is negative.

The Fermi-contact term is often simplified⁹ by neglecting two-center contributions. However, Pachler¹² has shown that inclusion of two-center contributions results in calculated couplings which differ by up to 20% from those obtained with simplified calculations. Because substituent effects may well be as large, it was decided, following Pachler,¹² to include all one- and two-

(7) Hoffmann, R. *J. Chem. Phys.* **1963**, *39*, 1397.

(8) Ramsey, N. F. *Phys. Rev.* **1953**, *91*, 303.

(9) Pople, J. A.; Santry, D. P. *Mol. Phys.* **1964**, *8*, 1.

(10) Barbier, C.; Faucher, H.; Berthier, G. *Theor. Chim. Acta* **1971**, *21*, 105.

(11) McConnell, H. M. *J. Chem. Phys.* **1956**, *24*, 460.

(12) Pachler, K. G. R. *Tetrahedron* **1971**, *27*, 187.

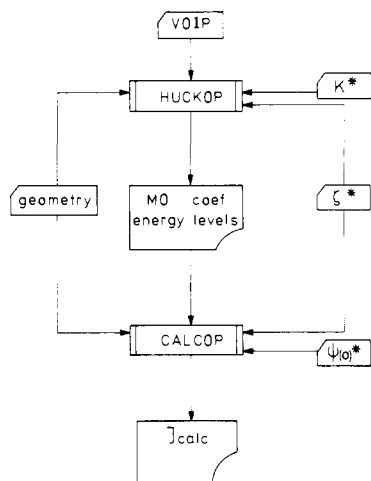


Figure 1. Schematic representation of the (noniterative) EHMO program. The optimized parameters are marked with an asterisk. For explanation of the symbols used, see text.

center integrals of the valence shell atomic orbitals in the calculations.

In the EHMO method the Hamiltonian matrix elements are approximated by using empirical valence orbital ionization potentials (VOIP). As changes in their values do not greatly alter the magnitudes of the calculated couplings,⁴ no attempts were made to optimize the VOIPs. Values given by Basch et al.¹³ were used throughout.

Within the EHMO framework the calculation of the off-diagonal elements has been a matter of dispute.¹⁴ Two approximations are commonly used, the Wolfsberg-Helmholtz approximation,^{3,12} eq 9, and the Cusachs approximation,^{15,16} eq 10. We

$$H_{ij} = \frac{1}{2}KS_{ij}(H_{ii} + H_{jj}) \quad (9)$$

$$H_{ij} = \frac{1}{2}S_{ij}(2 - |S_{ij}|)(H_{ii} + H_{jj}) \quad (10)$$

carried out test calculations for ^1H - ^1H and ^{13}C - ^1H couplings using either method. The Wolfsberg-Helmholtz eq 9 gave better overall correspondence between the calculated and experimental couplings and was adopted in our final procedure. The test calculations also demonstrated that the calculated couplings were sensitive to the value of the Wolfsberg-Helmholtz constant, K . This fact led us to include K as an adjustable parameter in the optimization procedure.

Next, the influence of charge iteration¹⁷ was investigated. Usually, charge iteration involves time-consuming EHMO calculations, repeated until self-consistent atomic charges are obtained for each molecular species under investigation. Such an approach is impractical when a large number of different molecular species are treated simultaneously. In order to assess the relative importance of charge iteration, an approach was explored in which iteration was avoided. In this approach the atomic charges were estimated according to the partial equalization of orbital electronegativity procedure of Gasteiger and Marsili,¹⁸ and then the diagonal elements in the Hamiltonian were calculated from the regressions for the VOIPs given by Basch et al.¹³ Test calculations showed no noticeable improvement over our standard method, and therefore this line of investigation was abandoned.

In summary, the following parameters were optimized in order to obtain the best fit between experimental and calculated coupling constants: Slater exponent (ζ), the valence shell densities ($\psi(0)$),

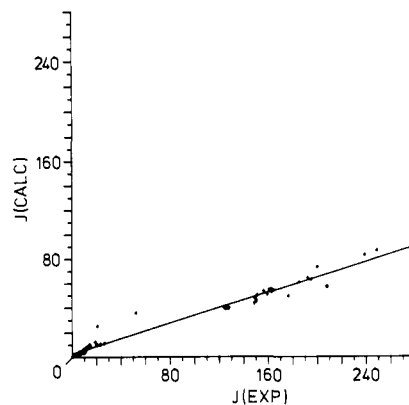


Figure 2. Observed and calculated coupling constants $^3J_{\text{HH}}$ and $^1J_{\text{CH}}$ (test data set, see text) using standard EHMO parameters.

and the Wolfsberg-Helmholtz constant (K). A schematic representation of the algorithm used for a single noniterative calculation is given in Figure 1. The subroutine HUCKOP determines the energy levels ϵ_i and the MO coefficients ci_λ and requires as input the molecular geometry, Slater exponents, Wolfsberg-Helmholtz constant, and the VOIPs. Additionally, in the subroutine CALCOP the $\psi(0)$ values and Slater exponents are read in and the actual calculation of the coupling constants is performed. The various adjustable input parameters are indicated in Figure 1 with an asterisk.

Optimum values of the adjustable parameters were determined by an iterative Newton-Raphson least-squares procedure using numerical first derivatives. The iteration process ceased when changes in root mean square deviation between observed and calculated coupling constants were less than one promille. Note that the Slater exponents of all atoms in the molecules were optimized, even when the atom is not directly involved in the coupling.

A number of trial calculations allowed the Slater exponents of the s and p valence orbitals of the heavy atoms to be optimized independently. These calculations indicated that differences in optimum values of s and p exponents were negligible in view of the estimated 90% confidence limits. Therefore, the constraint $\zeta_s = \zeta_p$ was used in all further calculations.

The data set used in the final optimization contained experimental couplings for a large number of molecules including alkanes, alkenes, and cycloalkanes with a variety of substituents, such as chlorine, fluorine, hydroxyl, and carboxyl groups. For small molecules experimental geometries were taken from Landolt-Börnstein¹⁹ whenever available, or else optimized ab initio geometries were used.^{20,21} Corrections for known differences^{20,21} between experimental and ab initio structures were applied. The structures of large molecules, e.g., *tert*-butylcyclohexane and 1,3-dimethylcyclohexane, were calculated by molecular mechanics²² using the force fields given by Ermer and Lifson²³ or by Allinger.²⁴

Results and Discussion

A representative test data set of 76 experimental couplings, containing both $^1J_{\text{CH}}$ and $^3J_{\text{HH}}$ values, was used for pilot calculations. In Figure 2 experimental and calculated coupling constants, using the original EHMO parameters given by Hoffmann, are shown. The calculated couplings are grossly underestimated; the root mean square (rms) deviation amounts to 73 Hz. After

(19) Landolt-Börnstein "Numerical data and Functional Relationships in Science and Technology"; Hellwege, K. H., Hellwege, A. M., Eds.; Springer Verlag: Berlin, 1976; Vol. 7.

(20) Blom, C. E.; Otto, L. P.; Altona, C. *Mol. Phys.* **1976**, *32*, 1137.

(21) Blom, C. E.; Slingerland, P. J.; Altona, C. *Mol. Phys.* **1976**, *31*, 1359. Blom, C. E.; Müller, A. *J. Mol. Struct.* **1978**, *46*, 93. Klimkowski, V. J.; Ewbank, J. D.; van Alsenoy, C.; Scarsdale, J. N.; Schäfer, L. *J. Am. Chem. Soc.* **1982**, *104*, 1476.

(22) Faber, D. H.; Altona, C. *Comput. Chem.* **1977**, *1*, 203.

(23) Ermer, O.; Lifson, S. *J. Am. Chem. Soc.* **1973**, *95*, 4121.

(24) Allinger, N. L. *Adv. Phys. Org. Chem.* **1976**, *13*, 1.

(13) Basch, H.; Viste, A.; Gray, H. B. *Theor. Chim. Acta* **1965**, *3*, 458.

(14) See, for example: Varga, J. A.; Zumdahl, S. S. *Theor. Chim. Acta* **1971**, *21*, 211.

(15) Cusachs, L. C. *J. Chem. Phys.* **1965**, *43*, S157.

(16) Carroll, D. G.; McGlynn, S. P. *J. Chem. Phys.* **1966**, *45*, 3827.

(17) Polezzo, S.; Cremaschi, P.; Simonetta, M. *Chem. Phys. Lett.* **1967**, *1*, 357.

(18) Gasteiger, J.; Marsili, M. *Tetrahedron* **1980**, *36*, 3219.

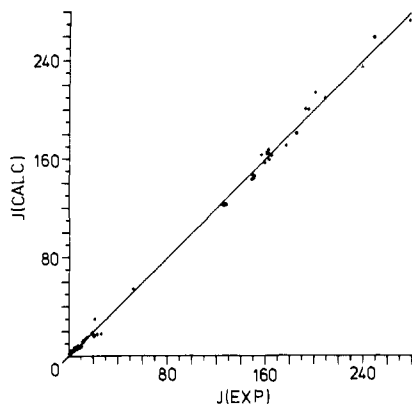


Figure 3. Observed and calculated coupling constants ${}^3J_{\text{HH}}$ and ${}^1J_{\text{CH}}$ (test data set, see text) using optimized EHMO parameters.

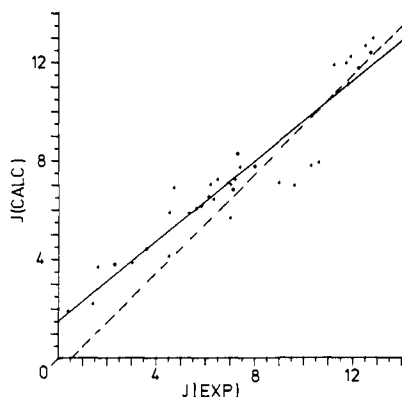


Figure 4. As in Figure 3, but only vicinal coupling constants ${}^3J_{\text{HH}}$ are shown: solid line, least-squares regression line calculated from observed and calculated vicinal couplings ranging from 0 to 14 Hz; dashed line, least-squares regression line resulting from complete test data set.

parameter optimization a good overall correspondence between experimental and calculated values was found. The final rms deviation reduces to 3.9 Hz; the slope and intercept of the least-squares regression line are 1.008 and -0.5 Hz, respectively, with a correlation coefficient of 0.999 (see Figure 3). However, a closer look reveals a de facto less satisfying situation. When vicinal and directly bonded couplings are examined separately, each subset shows systematic differences from the idealized regression line; see Figure 4, where an enlargement of Figure 3 showing only vicinal couplings ranging from 0 to 14 Hz is given. The least-squares regression line for the 3J subset is characterized by a slope of 0.81 and an intercept of 1.5 Hz. For the 1J subset these numbers are 1.05 and -8.1 Hz, respectively. Separate optimization of EHMO parameters for the subsets ${}^3J_{\text{HH}}$ and ${}^1J_{\text{CH}}$ was therefore performed.

Calculation of ${}^1J_{\text{CH}}$ and ${}^1J_{\text{CC}}$. The final EHMO parameters obtained from optimization on 61 experimental ${}^1J_{\text{CH}}$ coupling constants are presented in Table I. In Figure 5 the experimental couplings are compared with calculated values. The final rms deviation is 6.9 Hz. Comparison of the statistics obtained for the calculations using standard EHMO parameters⁷ with those for optimized parameters shows a large improvement in calculated coupling constants (Table I). Note that the optimization results only in small changes in the Wolfsberg–Helmholtz constant and Slater exponents. The increase in the hydrogen Slater exponent is in accordance with the findings of Murrell et al.²⁵ The optimized valence shell densities at the nucleus ($\psi^2(0)$) are substantially larger than the standard EHMO values.²⁶ This is not

(25) Murrell, J. N.; Stevenson, P. E.; Jones, G. T. *Mol. Phys.* **1967**, *12*, 265.

(26) As Slater-type functions are used, a straightforward calculation with standard EHMO parameters results in a zero value for the valence shell density at carbon. Therefore, the $\psi(0)$ value of carbon was chosen so that the integral $\psi^2(0)$ has the same value as that obtained with the use of hydrogen-like orbitals.

Table I. Optimized Values of Slater Exponents, Wolfsberg–Helmholtz Constant, and Valence Shell Densities for Calculation of ${}^1J_{\text{CH}}$ Coupling Constants and Statistics for a Least-Squares Straight-Line Regression Analysis of Calculated vs. Experimental Coupling Constants

parameter	this work	ref 7 ^a
K	1.7417	1.75
Slater exponents		
H	1.278	1.20
C	1.627	1.625
O	2.151	2.275
F	2.531	2.60
Cl	2.259	2.033
valence shell densities ^b		
H	0.849	0.742
C	-1.755	-1.169
statistics		
rms deviation, Hz	6.89	109
slope	1.014	0.367
intercept, Hz	-2.54	-2.98
correl coeff	0.984	0.951
no. of couplings	61	61

^a According to Hoffmann's EHMO parametrization (ref 7).

^b Given as $\psi(0)$ value (see text).

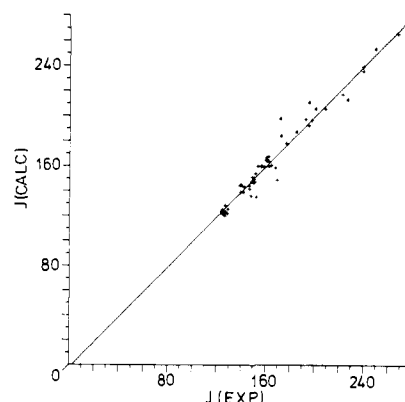


Figure 5. Observed and calculated ${}^1J_{\text{CH}}$ coupling constants using optimized EHMO parameters (Table I).

surprising because the necessity to increase the valence shell density at carbon for an improved description of experimental couplings is well-known, both in extended Hückel^{3,5,27} as in other semi-empirical calculations^{5,9,28,29} and may be associated with the neglect of 1s orbitals. The calculated couplings depend strongly upon the chosen $\psi(0)$ values as can easily be seen when the Fermi-contact contribution is approximated by eq 11. In the derivation of eq

$$J_{\text{AB}}^{\text{contact}} = (2\beta/3)h\gamma_A\gamma_B\psi_{0A}^2\psi_{0B}^2\pi_{\text{AB}} \quad (11)$$

11 only one-center integrals are retained; π_{AB} stands for the atom–atom polarizability of the s orbitals on A and B. The systematic underestimation of 1J values in the standard EHMO approach (vide supra) makes an increase in the hydrogen $\psi(0)$ value necessary.

A selection of experimental and calculated coupling constants, included in the data set, are presented in Table II. This table also presents ${}^1J_{\text{HC}}$ calculated by the INDO–FPT approximation³⁰ and by the CDOE/INDO LMO theory.³¹ In comparison with

(27) Fahey, R. C.; Graham, G. C.; Piccioni, R. L. *J. Am. Chem. Soc.* **1966**, *88*, 193.

(28) Pople, J. A.; McIver, J. W., Jr.; Ostlund, N. S. *J. Chem. Phys.* **1968**, *49*, 2965. Wray, V. J. *Am. Chem. Soc.* **1981**, *103*, 2503.

(29) Towl, A. D. C.; Schaumburg, K. *Mol. Phys.* **1971**, *22*, 49.

(30) Maciel, G. E.; McIver, J. W., Jr.; Ostlund, N. S.; Pople, J. A. *J. Am. Chem. Soc.* **1970**, *92*, 1.

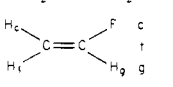
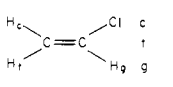
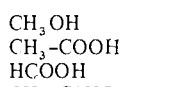
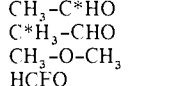
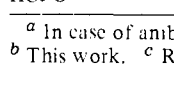

(31) van Alsenoy, C.; Figeys, H. P.; Geerlings, P. *Theor. Chim. Acta* **1980**, *55*, 87.

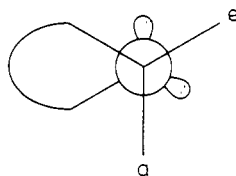
(32) Muller, N.; Pritchard, D. E. *J. Chem. Phys.* **1959**, *31*, 768, 1471.

(33) Frankiss, S. G. *J. Phys. Chem.* **1963**, *67*, 752.

(34) Watts, V. S.; Goldstein, J. H. *J. Phys. Chem.* **1966**, *70*, 3887.

Table II. Comparison of Observed and Calculated $^1J_{CH}$ Coupling Constants (Hz)^a

compd	J_{exptl}	J_{calcd}^b	J_{calcd}^c	J_{calcd}^d	ref
CH ₄	125.0	124.5	122.9		32
CH ₃ F	149.1	151.8	140.1	160.1	33
CH ₂ F ₂	184.5	187.8	166.8	193.0	33
CHF ₃	239.1	236.7	212.3	233.3	33
CH ₃ Cl	148.6	148.4			34
CH ₂ Cl ₂	176.5	178.6			34
CHCl ₃	208.1	206.3			34
CH ₃ -CH ₃	124.9	124.3	122.1	124.0	35
CH ₃ -C*H ₂ -CH ₃	125.3	123.4	119.4		36
CH ₃ -C*H ₂ Cl	150.0	147.8			36
CH ₃ -C*H ₂ OH	140.0	145.6			37
CH ₃ -C*H ₂ I	150.3	149.8	137.1	145.0	36
CH ₂ =CH ₂	156.2	160.1	156.7	161.6	35
CH=CH	248.7	254.3	232.7	242.9	38
CH=CF	277.5	271.8	251.5	274.6	39
CH ₂ =C=CH ₂	168.0	159.1	155.5	164.5	40
	159.2	159.7	153.3		41
	162.2	164.5	162.4		41
	200.2	206.4	183.1		41
	162.6	160.1			42
	160.9	164.7			42
	194.9	193.1			42
CH ₃ OH	142.0	139.4	135.3		43
CH ₃ -COOH	129.0	122.3	120.6	126.5	32
HCOOH	222.0	217.9	214.1	226.9	43
CH ₃ -C*HO	172.4	184.5	164.5	187.3	44
C*H ₃ -CHO	127.0	120.5	121.4	126.5	45
CH ₃ -O-CH ₃	139.6	139.5	135.5	148.9	33
HCFO	267.0	266.6	244.7	261.4	46

^a In case of ambiguity the coupling carbon atom is marked.^b This work. ^c Reference 30. ^d Reference 31.Figure 6. Newman projection along the O-C₁ bond in hexapyranoses giving a schematic representation of the oxygen lone pairs.

these methods, the present calculations give a lower rms deviation of the calculated from the experimental coupling constants.

For couplings included in Pople's data set³⁰ and our data set (28 couplings) the rms deviation drops from 12.8 to 7.8 Hz. With the data set of van Alsenoy³¹ 19 couplings are shared; in this case the rms deviation drops from 6.7 to 5.6 Hz. Table II reveals that the observed trends in couplings are closely followed by the calculated trends. The increase in experimental couplings when going from mono- to trisubstituted methanes is well reproduced.

(35) Lynden-Bell, R. M.; Sheppard, N. *Proc. R. Soc. London, Ser. A* **1962**, *A269*, 385.

(36) Spoormaker, T.; De Bie, M. J. A. *Recl. Trav. Chim. Pays-Bas* **1978**, *97*, 135.

(37) Spoormaker, T. Ph.D. Thesis, Utrecht, 1979.

(38) Graham, D. M.; Holloway, C. E. *Can. J. Chem.* **1963**, *41*, 2114.

(39) Shimonnin, M. P. *Bull. Soc. Chim. Fr.* **1966**, 1774.

(40) Whipple, E. B.; Goldstein, J. H.; Stewart, W. E. *J. Am. Chem. Soc.* **1959**, *81*, 4761.

(41) Mayo, R. E.; Goldstein, J. H. *J. Mol. Spectrosc.* **1964**, *14*, 173.

(42) Steiger, Th.; Gey, E.; Radeglia, R. *Z. Phys. Chem. (Leipzig)* **1976**, *257*, 172.

(43) Hammaker, R. M. *J. Mol. Spectrosc.* **1965**, *15*, 506.

(44) Malinowski, E. R.; Pollana, L. Z.; Larmann, J. P. *J. Am. Chem. Soc.* **1962**, *84*, 2649.

(45) Gray, G. A.; Ellis, P. D.; Traficante, D. D.; Maciel, G. E. *J. Magn. Reson.* **1969**, *1*, 41.

(46) Muller, N.; Carr, D. T. *J. Phys. Chem.* **1963**, *67*, 112.

Table III. Experimental and Calculated $^1J_{CC}$ Coupling Constants (Hz)^a

compd	exptl	contact	dipolar	orbital	total	ref
C*H ₂ -C*HCICH ₂	13.9	18.22	-0.48	-0.07	17.7	49
C*H ₂ -C*H ₂ CH ₃	33.2	31.17	0.17	0.04	31.4	1
CH ₃ -CH ₃	34.6	30.24	0.18	0.04	30.5	35
CH ₃ -CH ₂ OH	37.7	31.46	0.19	0.18	31.8	50
CH ₃ -CH ₂ I	38.2	36.02	0.30	0.18	36.5	1
C*H ₂ -C*HFCH ₃	39.1	35.35	0.27	0.19	35.8	51
CH ₃ -CHO	39.4	40.58	0.08	-0.09	40.6	45
CH ₂ =CH ₂	67.6	74.90	1.64	-3.97	72.6	38
C*H ₂ =C*HCH ₃	70.0	76.14	1.50	-3.73	73.9	49
C*H ₂ =C*CH ₂	98.7	91.10	1.48	-2.12	90.5	52
CH=CH	171.5	157.13	5.30	10.32	172.8	38

^a Calculations were performed by using the EHMO parameters obtained from optimization of $^1J_{CH}$ coupling constants (see Table I).

Table IV. Contributions from Different Mechanisms to the $^1J_{CC}$ Coupling Constants in Ethane, Ethene, and Ethyne

	contact	dipolar	orbital
C ₂ H ₆			
EHMO ^a	30.24	0.18	0.04
SOS INDO ^b	11.99	0.30	-0.55
LMO INDO ^c	27.2	0.2	-1.3
ab initio ^d	17.4	0.55	-0.04
SCPT INDO ^e	35.6	0.7	-2.9
C ₂ H ₄			
EHMO ^a	74.90	1.64	-3.97
SOS INDO ^b	29.75	0.93	-3.76
LMO INDO ^c	71.6	0.5	-3.2
ab initio ^d	69.2	3.67	-4.83
SCPT INDO ^e	70.6	3.9	-18.6
C ₂ H ₂			
EHMO ^a	157.13	5.30	10.32
SOS INDO ^b	69.43	2.84	4.13
LMO INDO ^c	141.1	2.2	1.4
ab initio ^d	190.7	0.35	1.89
SCPT INDO ^e	140.8	8.3	23.6

^a This work; parameters according to Table I. ^b Reference 29.

^c Reference 53. ^d Reference 10. ^e Reference 54.

The influence of an electronegative α -substituent in substituted ethanes is correctly calculated. In monosubstituted ethenes the calculated stereochemical dependence of the $^1J_{CH}$ coupling accords with experiment.

For compounds containing oxygen, trends in observed coupling constants are less well reproduced. In methanol the averaged calculated coupling is in fair agreement with the experimental value. However, from studies on hexapyranoses it is known that the orientation of the oxygen lone pairs has a significant influence on the directly bonded C-H coupling: the C-H coupling for an axial proton attached on C₁ (158-162 Hz) is smaller than the C-H coupling for an equatorial proton (169-171 Hz)⁴⁷ (see Figure 6). Extrapolating to methanol, one expects a relatively large coupling for the symmetrical hydrogen (in the plane of C-O-H) and smaller couplings for the asymmetric hydrogens. In the calculations a reversed trend is found: $^1J_{CH_1} = 127.8$ Hz and $^1J_{CH_2} = 145.1$ Hz. Similarly, in 2-methyl-1,3-dioxane experimental values⁴⁸ for the C₄-H₂ and C₄-H₃ couplings are 148.0 and 139.1 Hz, respectively, whereas the calculated values are 136.6 and 145.0 Hz. These examples are limited to anomeric situations. The symmetrical C-H distance in methanol is known to be shorter than the

(47) Bock, K.; Lundt, I.; Pedersen, C. *Tetrahedron Lett.* **1973**, 1037.

(48) Haasnoot, C. A. G., unpublished results.

(49) Stothers, J. B. ¹³C NMR Spectroscopy; Academic Press: New York, 1972.

(50) Gray, G. A. Ph.D. Thesis, University of California, 1967.

(51) Spoormaker, T.; de Bie, M. J. A. *Recl. Trav. Chim. Pays-Bas* **1979**, *98*, 380.

(52) Bertrand, R. D.; Grant, D. M.; Allred, E. L.; Hirshaw, J. C.; Strong, A. B. *J. Am. Chem. Soc.* **1972**, *94*, 997.

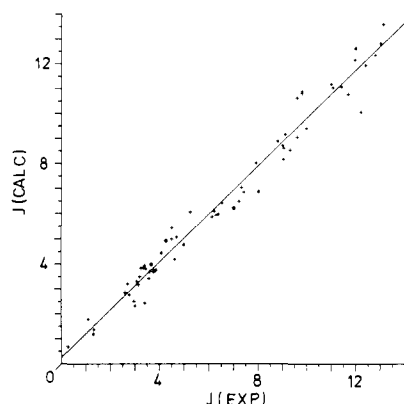


Figure 7. Observed and calculated ${}^3J_{\text{HH}}$ coupling constants using optimized EHMO parameters (Table V).

Table V. Optimized Values of Slater Exponents, Wolfsberg-Helmholtz Constant, and Valence Shell Density for Calculation of ${}^3J_{\text{HH}}$ Coupling Constants and Statistics for a Least-Squares Straight-Line Regression Analysis of Calculated vs. Experimental Coupling Constants

parameter	this work	ref 7 ^a
K	2.222	1.75
Slater exponents		
H	1.223	1.20
C	1.708	1.625
O	2.763	2.275
F	2.988	2.60
Cl	2.325	2.033
valence shell densities ^b		
H	0.949	0.742
statistics		
rms deviation, Hz	0.58	2.38
slope	0.975	0.632
intercept, Hz	0.18	0.65
correl coeff	0.989	0.984
no. of couplings	70	70

^a According to Hoffmann's EHMO parametrization (ref 7).

^b Given as $\psi(o)$ value (see text).

asymmetrical bond distance.²⁰ The structures used in the present calculations had not been corrected for this shortening and this problem was studied further by means of additional calculations. When the symmetrical C-H bond is foreshortened by 0.007 Å only a slight increase (ca. 0.5 Hz) in the symmetrical and a slight decrease (ca. 0.1 Hz) in the asymmetrical coupling is calculated. This improvement is far too small to cause a reversal of the calculated trend. Therefore bond foreshortening cannot remedy the problem encountered in anomeric situations. Evidently, the EHMO theory fails for an anomeric proton.

Although one-bond C,C couplings were not used in optimization of the EHMO parameters, ${}^1J_{\text{CC}}$ values are calculated in good correspondence with experiment (see Table III). The three contributions to the coupling constants are listed separately in Table III. For ${}^1J_{\text{CC}}$ couplings the Fermi-contact term remains the dominant contribution, but inclusion of the orbital and dipolar terms improves the correspondence between experimental and calculated values.

The contributions to the coupling constants are not readily comparable with results quoted in other theoretical papers^{10,29,53,54} because different levels of sophistication and different integral parametrization are used. Nevertheless, from Table IV it can be seen that the calculated contributions using the present method accord reasonably well with the values obtained by the other methods.

Calculation of ${}^3J_{\text{HH}}$. The results for ${}^3J_{\text{HH}}$ are presented in Table V and in Figure 7. The final rms deviation is 0.58 Hz for a data

Table VI. Comparison of Observed and Calculated ${}^3J_{\text{HH}}$ Coupling Constants (Hz)

compd	J_{exp}	J_{calcd}^a	J_{calcd}^b	ref
CH ₃ -CH ₃ ^c	8.0	6.9	8.4	35
CH ₃ -CH ₂ F ^c	7.0	6.2	7.4	36
CH ₃ -CHF ₂ ^c	4.5	5.0	5.9	55
CH ₃ -CH ₂ Cl ^c	7.2	6.5		36
CH ₃ -CHCl ₂ ^c	6.1	5.9		56
CH ₃ -CH ₂ OH ^c	7.0	6.2	7.7	57
CH ₃ -CH ₃ -CH ₃ ^c	7.4	6.9	8.1	36
CH ₃ -CHCl-CH ₃ ^c	6.5	6.4		36
CH ₃ -CHF-CH ₃ ^c	6.2	6.1		36
CH ₂ =CH ₂ (trans)	19.1	19.3	25.2	38
CH ₂ =CHCl (trans)	14.6	15.0		41
CH ₂ =CHF (trans)	12.8	12.4	20.7	59
CH ₂ =CH ₂ (cis)	11.5	10.8	9.3	38
CH ₂ =CHCl (cis)	7.3	7.1		41
CH ₂ =CHF (cis)	4.7	5.1	4.7	59
CH=CH ^d	9.5	7.1		58
cyclohexane				
aa	13.1	13.6	18.0	60
ac	3.7	4.0	2.7	60
ee	3.0	2.5	3.1	60
tert-butylcyclohexane				
1a2a	12.0	12.2		61
1a2e	3.1	3.3		61
2e3a	3.6	3.7		61
3a4e	3.8	3.8		61
3e4a	3.8	3.7		61
cyclohexanol				
1a2a	11.4	11.1		62
1a2e	4.2	5.0		62
trans-1,2-dihydrocyclohexane				
2a3e	4.5	5.5	3.4	63
2a3a	11.0	11.2	16.4	63
1,4-dioxane				
cis ^e	2.8	2.8		64
trans ^c	6.3	6.0		64
tert-butyl-1,3-dioxane				
4a5e	2.6	2.9		65
4a5a	12.4	12.0		65
4e5e	1.3	1.2		65
4e5a	5.0	4.8		65

^a This work. ^b Reference 66. ^c Time-average coupling. ^d Not included in parametrization.

set containing 70 experimental couplings. Comparison of the statistics of this minimization with the statistics obtained by using standard EHMO parameters shows an impressive improvement in calculated couplings.

Changes in the EHMO parameters during optimization are larger than for ${}^1J_{\text{CH}}$ couplings. Perhaps this is related to the increase in distance between the coupled nuclei. A comparison of some observed and calculated couplings used in the parametrization is given in Table VI, together with values from the INDO/FPT method.⁶⁶ For substituted ethanes experimental values are reproduced by both methods with nearly the same accuracy. However, for ethenes and cyclohexanes the EHMO method appears superior to the INDO/FPT method.

With the present method, in monosubstituted ethanes and gem-disubstituted propanes the observed decrease in conforma-

(55) Flynn, G. W.; Baldeschwieler, J. D. *J. Chem. Phys.* **1962**, *37*, 2907.

(56) Sheppard, N.; Turner, J. J. *Proc. R. Soc. London, Ser. A* **1959**, *A252*, 506.

(57) Bothner-By, A. A.; Glick, R. E. *J. Chem. Phys.* **1956**, *25*, 362.

(58) Denis, A.; Malrieu, J.-P. *Mol. Phys.* **1972**, *23*, 581.

(59) Banwell, C. N.; Sheppard, N. *Discuss. Faraday Soc.* **1962**, *34*, 115.

(60) Garbisch, E. W., Jr.; Griffith, M. G. *J. Am. Chem. Soc.* **1968**, *90*, 6543.

(61) Haddon, V. R.; Jackman, L. M. *Org. Magn. Reson.* **1973**, *5*, 333.

(62) Anet, F. A. L. *J. Am. Chem. Soc.* **1962**, *84*, 1053.

(63) Lemieux, R. V.; Lown, J. W. *Tetrahedron Lett.* **1963**, 1229.

(64) Smith, W. B.; Shoulders, B. A. *J. Phys. Chem.* **1965**, *69*, 579.

(65) Buys, H. R.; Eliel, E. L. *Tetrahedron* **1970**, 2779.

(66) Maciel, G. E.; McIver, G. W., Jr.; Ostlund, N. S.; Pople, J. A. *J. Am. Chem. Soc.* **1970**, *92*, 4497.

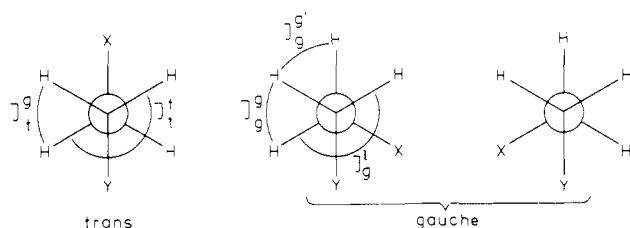
(53) Hirao, K.; Kato, H. *Bull. Chem. Soc. Jpn.* **1977**, *50*, 303.

(54) Blizzard, A. C.; Santry, D. P. *J. Chem. Phys.* **1971**, *55*, 950; *Ibid.* **1973**, *58*, 4714.

Table VII. Comparison of Coupling Constants (Hz) for the Rotamers in 1,2-Disubstituted Ethanes Calculated from the EHMO Theory^a and from the Linear Regressions Given by Abraham and Gatti^b

compd	method	J_t^g	J_t^t	J_g^g	$J_g^{g'}$	J_g^t	$\Sigma J_g^t + J_g^{g'}$	ϕ_X^c	$\Sigma \chi_i^d$
CH ₂ F-CH ₂ F	FHMO	5.01	11.37	2.65	1.23	10.40	11.63	60	7.8
	EHMO			1.54	2.19	9.24	11.43	70	
	AG	6.3	11.2	1.6	-0.7	11.8	11.1		
CH ₂ F-CH ₂ Cl	EHMO	4.81	11.80	2.88	1.48	11.28	12.76	60	7.05
	FHMO			2.24	1.98	10.84	12.82	65	
	AG	5.8	11.9	2.3	0.4	12.2	12.6		
CH ₂ Cl-CH ₂ Cl	EHMO	4.56	12.35	3.03	1.83	12.08	13.91	60	6.3
	EHMO			2.35	2.42	11.73	14.15	65	
	AG	5.3	12.5	3.0	1.4	12.7	14.1		

^a Using optimized parameters (Table V). ^b Reference 67. ^c X-C-C-Y (X, Y = F, Cl) torsion angle in gauche rotamer. ^d Sum of the electronegativity of X and Y on the Huggins' scale.⁷²

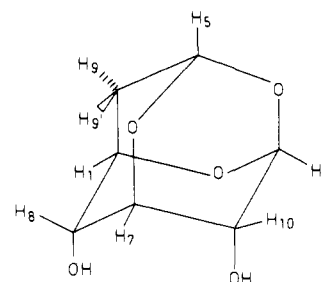
**Figure 8.** Rotational isomers of 1,2-disubstituted ethanes.

tionally averaged coupling due to electronegative substituents is reproduced, although the experimental decrease appears to be more marked. In cyclohexane a close agreement between experiment and theory is found. In 2-*tert*-butyl-1,3-dioxane the calculated differences in the gauche couplings, which arise mainly from the different orientation of electronegative substituents with respect to the coupling nuclei,⁶⁷⁻⁶⁹ are consistent with experiment.

The experimental couplings in mono- and 1,1-disubstituted ethanes used in the data set represent time-average values, and a direct comparison between observed and calculated trans and gauche couplings is precluded in these series. However, a limited comparison can be carried out for 1,2-disubstituted ethanes. From the solvent dependence of the vicinal couplings Abraham and Gatti⁶⁷ (A-G) were able to estimate values of J_t^t , J_t^g , and J_g^g and of the sum $J_g^{g'} + J_g^t$ for the pure rotamers (see Figure 8, the subscript indicates the relative gauche (g) or trans (t) orientation of the vicinal substituents, the superscript that of the coupled protons). A-G⁶⁷ derived separate estimates of J_g^g and J_g^t with the aid of data obtained from some six-membered ring compounds. Finally, each of the five coupling types mentioned above was shown to be linearly correlated with the sum of the electronegativities of the substituents. The most interesting aspect of this work⁶⁷ was that each of the linear regressions had a different slope; four of the J 's decreased with increasing electronegativity, whereas J_g^g displayed the reverse trend, contrary to previously held views.

The present EHMO calculations not only reproduce the observed trends but also help to clarify some ambiguities in connection with the A-G data. These concern the geometry of the gauche conformers, and the validity of the separate estimation of $J_g^{g'}$ and J_g^t . These problems are intimately related.

Table VII displays the couplings for the trans and gauche rotamers of 1,2-difluoro-, 1,2-dichloro-, and 1-chloro-2-fluoroethane, calculated by means of the EHMO method. These results are compared with the couplings obtained from the AG linear regressions.⁶⁷ Taking the approximations inherent to the AG method into account, it is seen that J_t^t is reproduced very well, J_t^g somewhat less so. Because the geometry of the trans conformer can be taken as 180°, the differences between observed and calculated J_t^g cannot have a geometrical origin. The discrepancy may arise from the strong bias toward the gauche conformer in the difluoro compound. Therefore, the properties of the trans

**Figure 9.** Structure of 8(a),10(a)-dihydroxy-2,4,6-trioxadamantane and labeling of protons.

rotamer are subject to a larger uncertainty than are those of the gauche rotamer.

The true geometries of the gauche rotamers of the 1,2-dihaloethanes in solution are not known with precision. However, accurate electron-diffraction results are now available for gauche 1,2-difluoroethane in the gas phase.^{70,71} It is found that $\phi_{FCCF} = 71-72^\circ$, appreciably larger than the classical gauche angle. For this reason the EHMO calculations were carried out for $\phi_{XCCY} = 60^\circ, 65^\circ, 70^\circ$, and 75° . Representative results are also shown in Table VII. For J_g^g we find satisfactory agreement with the AG data⁶⁷ using the following torsion angles: 60° for 1,2-dichloro-, 65° for 1-chloro-2-fluoro-, and 70° for 1,2-difluoroethane. The experimentally accessible sum of the couplings $J_g^t + J_g^{g'}$ is also well reproduced by the EHMO calculations. It should be noted that this sum is predicted to be virtually independent of the chosen geometry. Matters are different, however, for the individual couplings J_g^g and J_g^t , formally equivalent to an ee, aa pair in six-membered rings.

In all three 1,2-dihaloethanes $J_g^g(\text{calcd}) > J_g^g(\text{regression})$ and $J_g^t(\text{calcd}) < J_g^t(\text{regression})$; moreover, the discrepancy increases on going from dichloroethane via chlorofluoroethane to difluoroethane. Clearly, the reason for the discrepancy should be sought in the geometrical difference between six-membered rings in the chair form ($\phi_{XCCY} \sim 55^\circ$) and 1,2-dihaloethanes ($\phi_{XCCY} \geq 60^\circ$). This difference would invalidate the separate estimation of $J_g^{g'}$ and J_g^t with the aid of data derived from 1,1,4,4-tetra-deuteriocyclohexane, morpholine, and *trans*-2,3-dimethyl-1,4-dioxane, as was done by A-G.⁶⁷ It is easily seen that closure of the ϕ_{XCCY} angle in ring compounds results in a widening of the opposing H-C-C-H torsion and therefore in an appreciable decrease of J_{ee} relative to J_g^g in open-chain compounds. The A-G regression of J_g^t was derived by subtraction and this procedure then automatically leads to an overestimate. It now appears that the EHMO method offers a more reliable separation of $J_g^{g'}$ and J_g^t than was previously possible. The EHMO predictions for classical gauche angles are given in eq 12 and 13, where χ_x and χ_y are the electronegativities on the Huggins' scale.⁷²

$$J_g^g(60) = 4.33 - 0.40(\chi_x + \chi_y) \quad (12)$$

$$J_g^t(60) = 19.15 - 1.12(\chi_x + \chi_y) \quad (13)$$

(67) Abraham, R. J.; Gatti, G. *J. Chem. Soc. B.* **1969**, 961.

(68) Altona, C.; Haasnoot, C. A. G. *Org. Magn. Reson.* **1980**, *13*, 417.

(69) Haasnoot, C. A. G.; de Leeuw, F. A. A. M.; Altona, C. *Tetrahedron* **1980**, *36*, 2783.

(70) Fernholt, L.; Kveseth, K. *Acta Chem. Scand., Ser. A* **1980**, *A34*, 163.

(71) Friessen, D.; Hedberg, H. *J. Am. Chem. Soc.* **1980**, *102*, 3987.

Table VIII. Comparison of Experimental and Calculated $^3J_{\text{HH}}$ Coupling Constants (Hz) in 8(a),10(a)-Dihydroxy-2,4,6-trioxadadamantane (See Figure 9)

coupling	J_{exptl}^a	J_{calcd}
1-8	1.4	2.0
1-9	4.8	3.7
1-9'	1.5	1.4
3-10	1.9	2.5
5-9	2.7	2.2
5-9'	2.4	2.3
7-8	4.0	4.2
7-10	3.9	3.7

^a Experimental couplings taken from ref 73.

As a final test of the predictive power of the present EHMO parameters, coupling constant calculations on 8(a),10(a)-dihydroxy-2,4,6-trioxadadamantane were carried out (Figure 9, Table VIII). This compound is well suited for this purpose, because it has a rigid geometry and contains a number of suitably placed electronegative oxygen atoms. Thus, the combined effect of anti, gauche, and geminal oxygens upon various couplings can be studied. Table VIII shows excellent agreement between observed⁷³

(72) Huggins, M. L. *J. Am. Chem. Soc.* **1953**, *75*, 4123.

and calculated couplings. The rms deviation is nearly equal to the final rms deviation obtained for the data set used in the derivation of the EHMO parameters.

Conclusion

In this paper new parameter sets for the EHMO model are given, optimizing the agreement between calculated and observed $^1J_{\text{CH}}$ and $^3J_{\text{HH}}$ couplings. With the use of these parameter sets, a host of experimental trends due to substituent or stereochemical effects are reproduced by the calculations. In combination with the relatively small amount of computer time and storage needed for the EHMO calculations, this approach allows accurate theoretical studies concerning the various factors that influence the magnitude of coupling constants with the aim of incorporating these factors in practically useful relationships between coupling constants and geometrical factors such as the generalized Karplus equation.⁶⁹

Acknowledgment. We thank Dr. M. C. van Hemert for valuable suggestions in setting up the computer programs. We are indebted to Dr. A. H. Huizer for many helpful discussions and to a referee for many stylistic improvements.

(73) Jochims, J. C.; Taigel, G.; Meyer zu Reckendorf, W. *Tetrahedron Lett.* **1967**, 3227.

Preferential Solvation of Hydrogen Ions in Mixed Water-Amine Ion Clusters

A. J. Stace*

Contribution from the Department of Chemistry, The University, Southampton, Hants SO9 5NH, U.K. Received August 11, 1983

Abstract: A combined molecular beam-mass spectrometer apparatus has been used to generate mixed water-amine ion clusters of the general form $\{(A)_n \cdot (H_2O)_m\}H^+$ for $n + m \leq 18$ and for A equal to one of the following: NH_3 , CH_3NH_2 , $(CH_3)_2NH$, $(CH_3)_3N$, $CH_3CH_2NH_2$, $(CH_3CH_2)_2NH$, $(CH_3CH_2)_3N$, $CH_3CH_2CH_2NH_2$, or C_5H_5N (pyridine). By monitoring the competitive decomposition processes via metastable peak intensities, it has been possible to produce a qualitative picture of the primary, secondary, and tertiary solvation shells surrounding the proton. Despite the nonequilibrium nature of the experiment, the proposed solvent structure surrounding a proton in mixed water-ammonia ion clusters is in qualitative agreement with equilibrium thermodynamic results from the high-pressure mass spectrometry experiments of Kebarle et al. and Castleman et al. In mixed ion clusters containing either a primary or a secondary amine, the hydrogen ion is attached to a primary solvation shell composed of amine molecules. We have called these proton solvation units. In the secondary solvation shells surrounding these units it is found that both water and amine molecules compete for the available hydrogen-bonding sites. In the tertiary solvation shell water alone is the preferred solvent. This transition in solvent preference is rationalized in terms of a gradual decline in the ability of the proton to contribute to the formation of charge-enhanced hydrogen bonds as the size of the cluster increases. In order to account for the observed behavior of the tertiary alkylamine and pyridine mixed ion clusters, a series of structures with protonated water molecules contained within an amine shell are proposed. The possible significance of these structures in selective ion sequestering is discussed. In almost every example studied the number of available hydrogen-bonding sites appears to play a major role in determining the size, shape, and constitution of the solvation shells. The relationship between basicity of the amine and the proposed solvent structures is also discussed.

The protonation of amines in dilute aqueous acid has been the subject of numerous experimental¹⁻⁷ and theoretical⁸⁻¹⁷ papers. Of particular interest in many of these studies has been the effect alkyl substitution has on the irregular ordering of the basicities (pK_a 's). By combining quantitative results on gas-phase basicities with accurate solution thermochemical measurements, it has been possible to separate the bulk protonation data for a number of amines into molecule-dependent and solvent-dependent terms.¹⁸⁻²⁶ Because gas-phase measurements of both the proton affinities and the basicities²⁷ have established the order $NH_3 < CH_3NH_2 <$

$\{CH_3\}_2NH < \{CH_3\}_3N$ for the proton-acceptor abilities, it has generally been concluded that anomalies in the pK_a 's arise from

- (1) Everett, D. H.; Wynne-Jones, W. F. K. *Proc. R. Soc. London, Ser. A* **1940**, *A177*, 499.
- (2) Trotman-Dickenson, A. F. *J. Chem. Soc.* **1949**, 1293.
- (3) Evans, A. G.; Hamann, S. D. *Trans. Faraday Soc.* **1951**, *47*, 34.
- (4) Pearson, R. G.; Vogelsong, D. C. *J. Am. Chem. Soc.* **1958**, *80*, 1038.
- (5) Clark, J.; Perrin, D. D. *Q. Rev. Chem. Soc.* **1964**, *18*, 295.
- (6) Christensen, J. J.; Izatt, R. M.; Wrathall, D. P.; Hansen, L. D. *J. Chem. Soc. A* **1969**, 1212.
- (7) King, E. J. "Acid Base Equilibria"; Pergamon Press: New York, 1965.
- (8) Hehre, W. J.; Pople, J. A. *Tetrahedron Lett.* **1970**, *34*, 2959.
- (9) Lathan, W. A.; Hehre, W. J.; Curtiss, L. A.; Pople, J. A. *J. Am. Chem. Soc.* **1971**, *93*, 6377.

* Present address: School of Molecular Sciences, University of Sussex, Falmer Brighton, Sussex BN1 9RH, U.K.